Advanced Journal of Chemistry, Section A, 2026, 9(7), 1337-1347

Advanced Journal of Chemistry, Section A

Journal homepage: www.ajchem-a.com

Original Research Article

Theoretical Simulation of Oil Pollutant Adsorption: Diesel Interactions with Polyethersulfone Membranes

Hossein Nourmohamadi[1]*, Razieh Sadat Neyband[2]

[1]*Mineral Elements Group, Department of Advanced Materials and New Technologies, Iranian Research Organization for Science and Technology (IROST), Tehran, Iran*
[2]*Department of Physical Chemistry, Faculty of Chemistry, Lorestan University, Khorramabad, Iran*

ARTICLEINFO

Article history

Submitted: 2025-08-24
Revised: 2026-01-27
Accepted: 2026-02-18
ID: AJCA-2508-1910
DOI: 10.48309/AJCA.2026.526710.1910

KEYWORDS

Polyethersulfone membranes
Diesel adsorption
Molecular simulation
Oil pollutants
Solubility parameters

ABSTRACT

This study examines the interactions between diesel molecules and polyethersulfone (PES) membranes, focusing on the mechanical properties, adsorption behavior, and thermodynamic characteristics of different crystal surfaces. The results demonstrate that the (001) surface exhibits stronger binding energy and a higher electron density near the Fermi level compared to the (100) surface, indicating greater surface reactivity. Cohesive energy density analysis reveals that the electrostatic-to-van der Waals energy ratio for the (001) surface (9:1) is substantially higher than that of the (100) surface (approximately 7:4), reflecting enhanced electron exchange interactions. In addition, shear energy analysis indicates lower shear resistance on the (001) surface, suggesting increased surface instability in the presence of diesel molecules. Notably, diesel molecules aligned parallel to the PES aromatic rings exhibit significantly stronger adsorption, leading to improved pollutant capture and enhanced oil–water separation performance. However, excessively strong interactions may limit further pollutant adsorption and increase the risk of membrane clogging, highlighting the importance of balancing adsorption strength and membrane stability in PES membrane design.

GRAPHICAL ABSTRACT

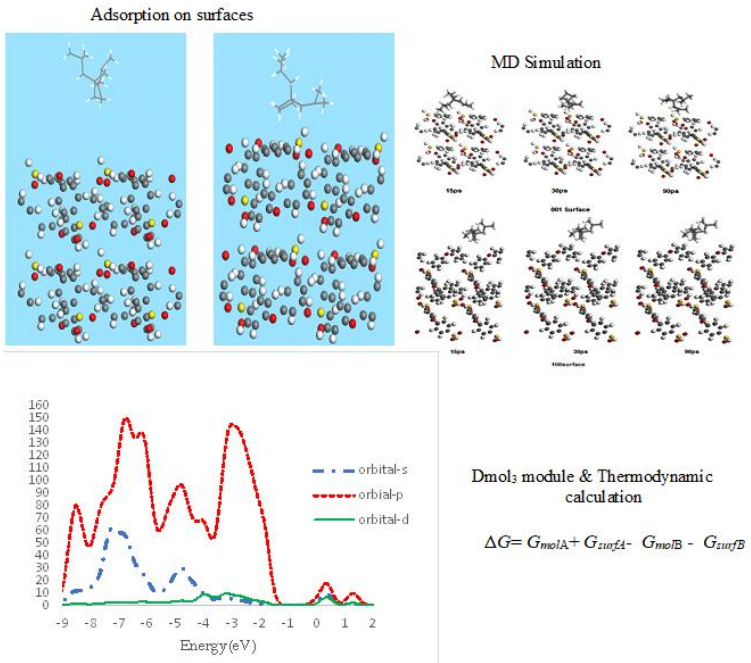

* Corresponding author: Nourmohamadi, Hossein
✉ E-mail: h_nourmohamadi@irost.ir

Introduction

Freshwater scarcity and the global water crisis pose significant challenges, particularly in underdeveloped regions. A major contributor to this issue is the generation of oily wastewater from various industrial processes, including food processing, metallurgy, petrochemical operations, and oil refineries [1,2]. The discharge of such wastewater can lead to severe environmental pollution and the depletion of vital water resources [3]. Furthermore, reports indicate that persistent hydrophobic oily residues can contaminate agricultural soils, often rendering them hydrophobic and significantly reducing water infiltration capacity [4]. Current approaches for treating oily wastewater primarily involve physical and chemical methods [5]. However, separating water and oil emulsions for microemulsions containing stabilizing surfactants remains a challenge [6]. In addition, emulsion separation is more complicated than oil and water mixture separation [7]. Membrane technology is an efficient technique due to its ability to effectively remove oil droplets compared to current technologies [8-13]. Significantly, the membrane performance depends on the surface properties of the membrane, such as moisture, surface charge and pore size, surface roughness [14-17]. Among the membrane processes, polymer ultrafiltration membranes are one of the most effective methods for treating oily effluents compared to conventional separation methods, due to their high oil removal efficiency without the need for chemical additives and low energy costs [18]. Polymeric membranes include polysulfone (PSF), polyether sulfone (PES), polyvinylidene fluoride (PVDF), polyacrylonitrile (PAN) and cellulose acetate (CA) [8, 19-21].

Simple and complex metal oxide nanostructures including ZnO, NiO, CuO, Co_3O_4, Mn_3O_4, Mn_2O_3, and spinels (AB_2O_4) have unique properties due to their nanoscale dimensions that can be added to polymer membranes [22]. Chitosan is also a natural amino polysaccharide with unique structure and versatile properties that are widely used in the industry. Its combination with metal oxide nanoparticles imparts the chemical and surface properties of organic compounds [23]. The positive effect of adding metal oxide nanoparticles on the performance of composite membranes has also been mentioned in previous studies [24-28]. Yuliwati *et al.* used composite matrix membranes to purify oily wastewaters. They found that a 1.95% increase in TiO_2 nanoparticles for the membrane increased flux by about 82.5 and 98.83 % ($L.m^{-2}.h^{-1}$) oil recovery [24].

Diesel is composed primarily of straight-chain, branched-chain and alkanes, along with a portion of cycloalkanes and aromatic hydrocarbons. The length of the carbon chains typically ranges from C_{10} to C_{20} or more, resulting in a higher boiling point and energy density for diesel compared to gasoline. These chains make up about 70 to 80 percent of diesel and are long-chain hydrocarbons (alkanes). About 20 to 30 percent of the mixture consists of compounds such as derivatives of toluene or naphthalene (aromatics), along with smaller amounts of alkenes and sulfur-containing compounds (which are reduced in low-sulfur diesel) [29-31]. Some researchers have focused on the three-dimensional modeling of the structure of PES membranes and the examination of its structural effects on the absorption of pollutants [32,33]. Additionally, some studies have investigated PES modified membranes and their performance in absorbing oil-based pollutants. Furthermore, a comparison has been made between PES and other membrane materials concerning the absorption of oil pollutants using molecular simulations [34-36].

However, this study specifically addresses the adsorption of diesel emphasizing its alkane fraction as a key pollutant in the mining industry. It investigates the interaction of diesel with the surface of polyethersulfone (PES) membranes using molecular simulations, including molecular

dynamics (MD) and density functional theory (DFT), noting that no prior work has focused explicitly on this topic. Considering that alkane rings constitute the predominant component of diesel fuel, the study will focus on the adsorption of this class of structures on the membrane surface.

Computational details

All spin-unrestricted DFT calculations were performed by the DMol3 [37,38] module in Material Studio and computations were carried out in a water solvent using the conductor-like screening model (COSMO) [39] with a global cutoff value of 4 Å and smearing values of 0.005 Ha. The convergence criteria for energy, force, and displacement were set to 10-5 Ha, 0.001 Ha/Å, and 0.005 Å, respectively. The MD simulations were performed by the Forcite module in Materials Studio using the Compass force field [40]. The geometries were optimized using the maximum iteration of 500**,** with fine quality and an energy of convergence tolerance of 1×10^{-4} kcal/mol. The simulation steps were 1 fs, with a total dynamic time of 100.0 ps. A constant number of atoms, volume, and energy ensemble (NVE) was employed in this study at T=298.15 K with initial random velocities [41,42]. Additionally, the interaction energy was calculated according to Equation 1.

$$E_{ads} = E_{tot} - (E_{surf} + E_{mol}) \quad (1)$$

Where, E_{tot} is the total energy of the surface and the diesel molecule, E_{surf} corresponds to the energy of the surfaces, and E_{mol} is the energy of an isolated diesel molecule.

Results and Discussion

First, the PES structure based on a monomer was constructed and optimized. Afterward, using the amorphous cell module and creating the desired network from the prepared structure, (100, 001) surfaces were adapted and optimized. The surface of (100) was selected to investigate the interaction of diesel with the atoms of the PES ring, while the (001) surface was chosen to study how the diesel molecule interacts with the rings and the voids in the structure. Now, by inserting the optimized diesel molecule into the cell and selecting the In-cell option from the lattice window, the structures are prepared for calculations. The complex structures are shown in Figures 1 and 2. Considering that alkane rings constitute the predominant component of diesel, the study will focus on the adsorption of this class of structures (n-$C_{12}H_{24}$) on the membrane surface.

Using Equation 1, the adsorption energy of a diesel molecule on the (100, 001) surfaces is calculated to be −30 and −116 kcal/mol, respectively. The comparison of adsorption energies indicates a stronger interaction between the diesel molecule and the (001) surface. When the rings are oriented parallel to the pollutant, the likelihood of stronger interaction and adsorption on the surface is higher. In contrast, if the molecule is not aligned parallel to the surface-ring atoms and is instead in the empty space between the rings, in contact with the surrounding atoms (interacting), the adsorption becomes weaker, and the energy value decreases.

Tables 1 and 2 show the Hirshfeld atomic charges of the O, H, C, and S atoms of surfaces near the diesel molecule. A comparison of Tables 1 and 2 also shows that the charge variations for the (001) surface are greater than those for the (100) surface. Here, the presence of sulfur, in addition to oxygen on the surface, leads to an increase in electron exchange between the diesel molecule and the (001) surface. Consequently, the interaction in this case is greater than that for the (100) surface.

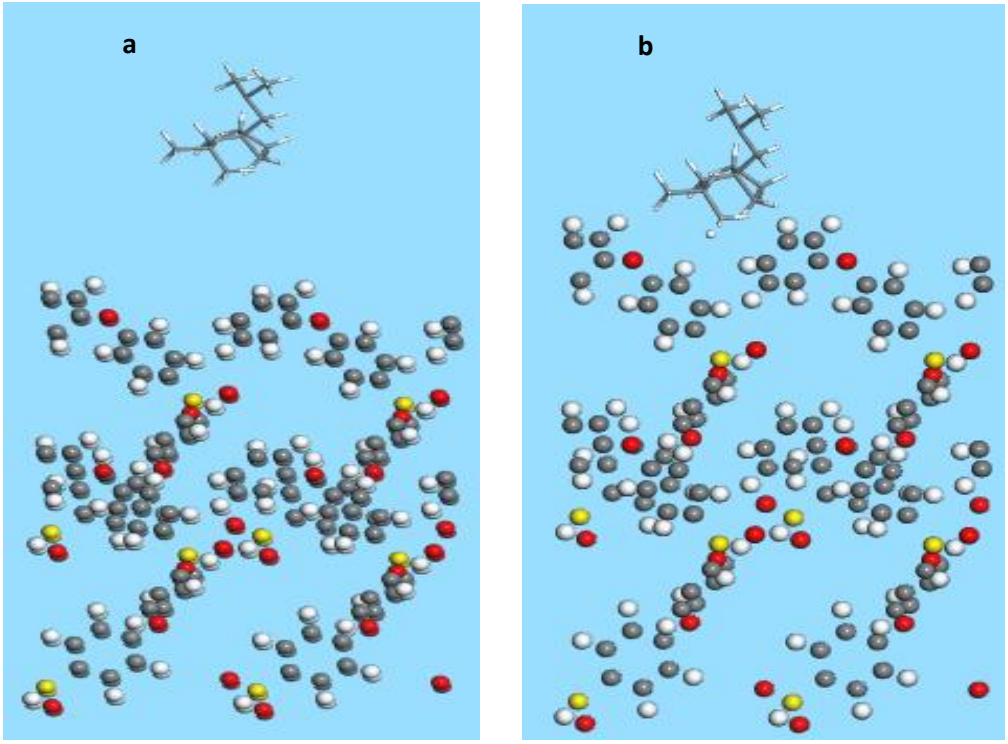

Figure 1. Diesel molecule and 100 surface; a. Initial location of diesel molecule above the surface and inside the constructed cell and b. diesel molecule adsorbed on the 100 surfaces

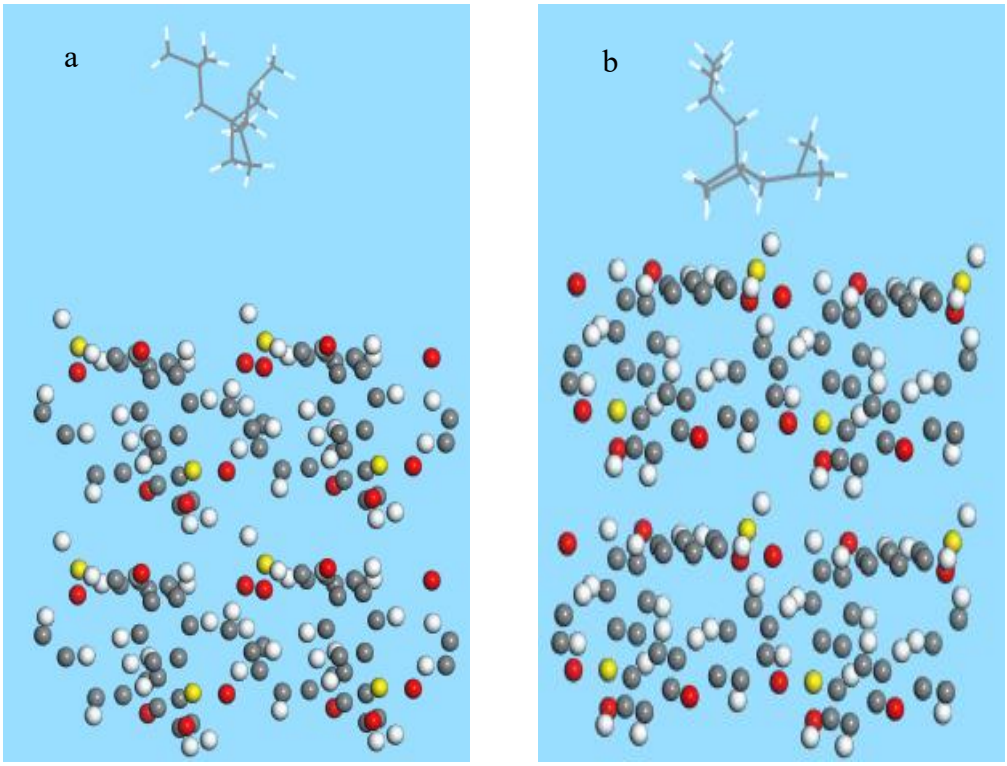

Figure 2. Diesel molecule and 001 surface; a. Initial location of diesel molecule above the surface and inside the constructed cell and b. diesel molecule adsorbed on the 001 surface

Table 1. The calculated Hirshfeld atomic charges (in e) of interacting atoms before and after the diesel adsorption

(100) Surface	Before	After
Oxygen	-0.535	-0.464
Hydrogen	0.127	0.127
Carbon	-0.126	-0.126

Table 2. The calculated Hirshfeld atomic charges (in e) of interacting atoms before and after the diesel adsorption

(001) Surface	Before	After
Oxygen	-0.535	-0.485
Hydrogen	0.193	0.082
Carbon	0.160	0.160
Sulfur	-0.717	-0.728

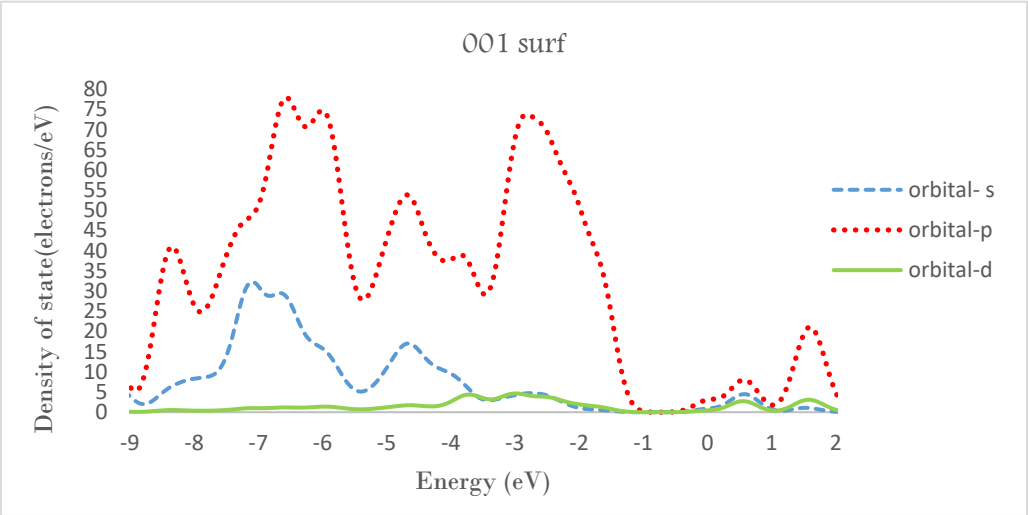

Figure 3. The PDOS diagram of s, p and d orbitals. 001 surface in contact with diesel molecule

Electron density studies were conducted in the context of electron transfer at the surface. As shown in Figures 3 and 4, the changes in electron density near the Fermi surface for the (001) surface are larger than those for the other surface. The density of the p-orbital state is generally higher and exhibits more distinct peaks than the d or s states, indicating that the p orbital plays a more active role relative to the other orbitals. It should also be noted that at higher (positive) energies, near the Fermi level, the p-orbital associated with the (001) surface is more active than that associated with the (100) surface. Based on Figure 4 and Table 1, the oxygen atom at the (100) surface shows the highest charge transfer to the diesel molecule and facilitates electron transfer from the surface to the p-orbitals of the diesel carbon. However, the p orbitals of the oxygen and sulfur atoms at the (001) surface, according to Table 2 and Figure 3, exchange electrons with the carbon p-orbital of the diesel molecule.

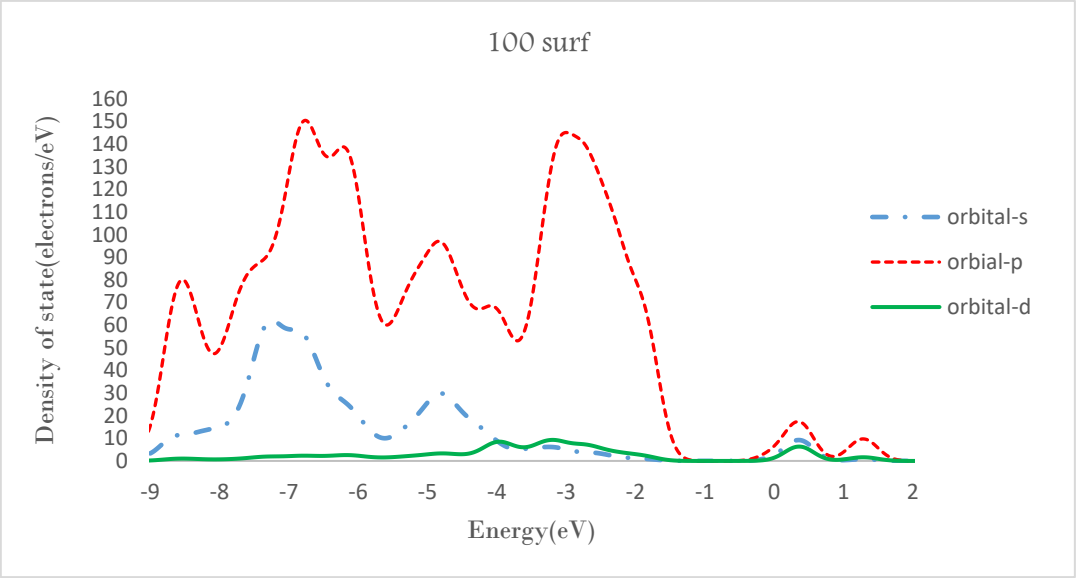

Figure 4. The PDOS diagram of s, p, and d orbitals. 001 surface in contact with diesel molecule

According to our DFT calculations, the free energy reaction was calculated using the following Equation [43]:

$$\Delta G = G_{molA} + G_{surfA} - G_{molB} - G_{surfB} \quad (2)$$

Where, G_{molB} and G_{molA} indicate the energy of an isolated diesel molecule before and after reaction with the surface, while the G_{surfB} and G_{surfA} terms correspond to the energy of PES surfaces (before and after interaction), respectively. The ΔG values for the (100) and (001) surfaces were obtained as − 45 and −186 kcal/mol, respectively. Considering these values, it can be concluded that the diesel molecule interaction over the titled surfaces is a thermodynamically spontaneous reaction. Moreover, it was found that the diesel interaction is more favorable with the (001) surface, and its free energy change is more negative over the (001) surface than over (100). Analysis of the binding energy density revealed that the energy value for the (001) surface is approximately double that of the (100) surface. Upon interaction with the (001) surface, the molecule exhibits an electrostatic-to-van der Waals energy ratio of 9:1, whereas this ratio is approximately 7:4 for the (100) surface. Enhanced electron exchange occurs between the diesel molecule and the (001) surface compared to the (100) surface, resulting in a stronger surface-pollutant interaction. Furthermore, the solubility parameter indicates greater stability when the molecule adsorbs onto the (001) surface, with corresponding energy values of 14.6 and 10.4 J/M^3 for the (001) and (100) surfaces, respectively. The contribution of electrostatic energy for the (001) surface is roughly twice that observed for the (100) surface.

Table 3. The shear modulus for the (100, 001) surfaces

Module	Layers	
	Surface (100)	Surface (001)
Shear module (GPa)	0.34	0.17

The mechanical structure of the surfaces after interaction with the diesel molecule was further investigated. It is expected that the shear energy of the (001) surface is relatively lower than that of the (100) surface. Images of the intermediate configurations obtained during the MD simulations, along with the potential energy as a function of time, are shown in Figures 5 and 6, which support this expectation. A contaminant

adsorbs onto (001) surface with a lower potential energy, and its subsequent reaction can proceed with the least activation energy. The reaction pathway on the (100) surface requires greater activation energy, or structural changes are needed to surmount a larger energy barrier. As a result, (001) surface shows a greater tendency to react with the pollutant, indicating its instability and reactivity compared to the (100) surface [44]. Additionally, the data in Table 3 also confirm that the shear energy of the (001) surface is lower than that of the (100) surface. In practice, the (100) surface is more stable when exposed to the diesel molecule, and its structure is preserved more effectively.

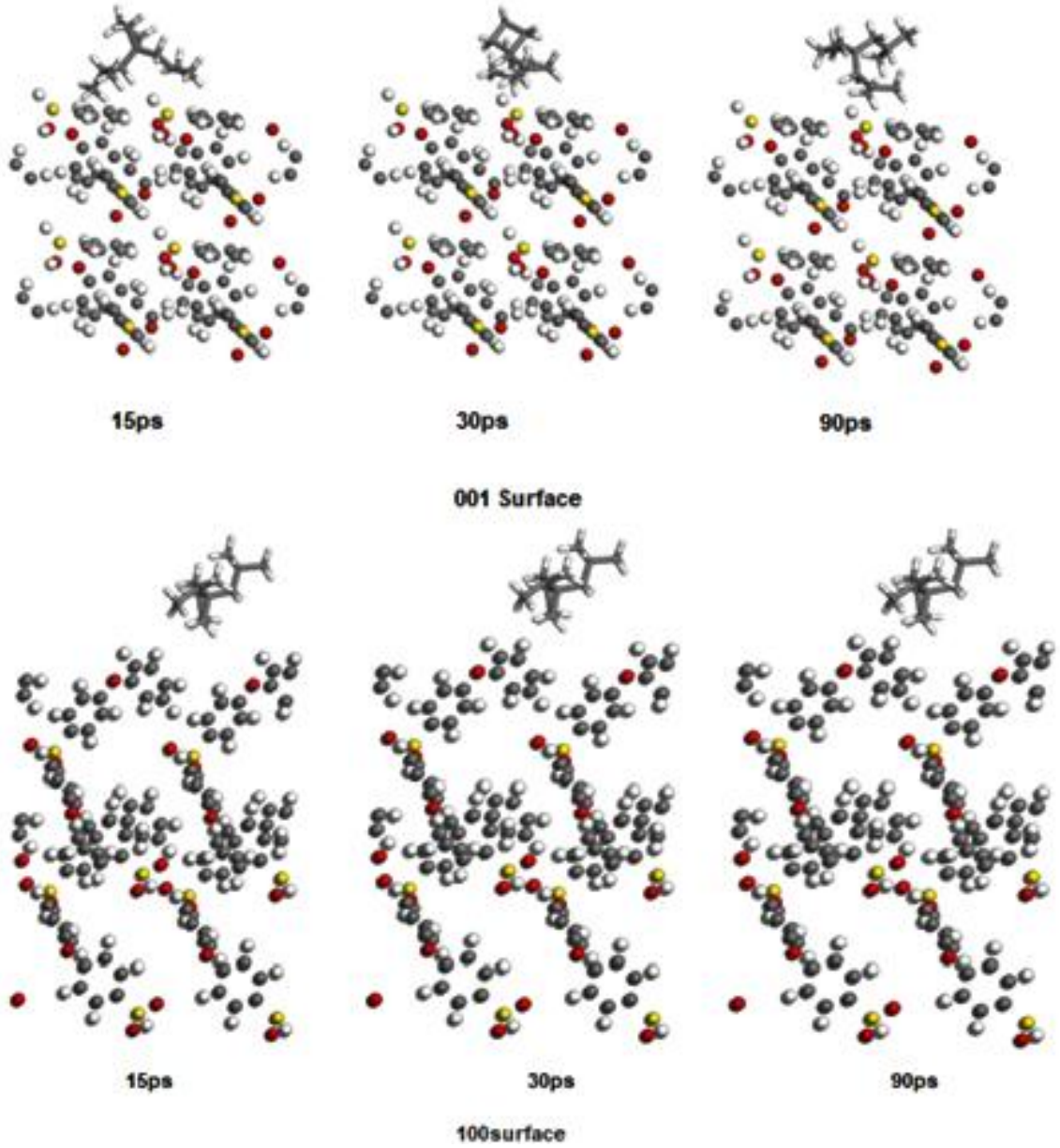

Figure 5. Snapshots for the NVE MD calculations, (001,100) surfaces with diesel

Figure 6. Graph of energy of each structure versus time for 100, 001 surfaces with diesel

From the studies conducted, it can be concluded that when the pollutant or diesel molecule is aligned parallel to the PES rings, stronger adsorption and more favorable interactions occur. Consequently, the pollutant is absorbed more efficiently by the membrane from the surrounding environment, thereby facilitating the oil–water separation. Nevertheless, a strong interaction between the pollutant and the membrane surface may reduce the membrane's capacity to absorb other pollutant molecules and can increase the likelihood of fouling within the PES rings, potentially affecting long-term membrane performance [45,46].

Conclusion

In summary, this study elucidates the interaction between diesel molecules and PES membranes, revealing how crystallographic orientation fundamentally governs membrane reactivity, stability, and separation performance. Unlike previous studies that primarily focus on bulk or macroscopic membrane properties, this work demonstrates that the (001) and (100) PES surfaces exhibit distinctly different electronic structures, cohesive energy distributions, and shear responses, which directly control pollutant–membrane interactions. This heightened activity,

however, stems from the surface's lower shear energy and greater instability. The superior adsorption performance of the (001) surface is shown to originate from enhanced electron exchange, higher electrostatic contributions, and lower shear resistance, enabling more effective oil–water separation. While, favorable for initial capture, the intense interaction can lead to rapid saturation, hindering the membrane's capacity for ongoing pollutant absorption and increasing the propensity for irreversible fouling and clogging. Consequently, the pursuit of maximum adsorption must be carefully weighed against long-term operational durability. Future designs should aim for a balanced interface that maintains sufficient affinity for targeted separation while mitigating excessive binding that compromises membrane lifespan. By mastering the intricate balance between reactivity and stability, more efficient, sustainable, and cost-effective solutions can be uncovered for water remediation and environmental protection. Ultimately, the insights bridge molecular-scale interactions with practical performance, guiding the next generation of membranes for complex separation challenges.

Acknowledgment

The authors would like to acknowledge the scientific support of the Iranian Research Organization for Science and Technology (IROST) for facilitating this research (Grants: 046048).

Disclosure Statement

No potential conflict of interest was reported by the authors.

ORCID

Hossein Nourmohamadi:
https://orcid.org/0000-0003-1463-0591
Razieh Sadat Neyband:
https://orcid.org/0009-0004-6592-6995

References

[1] Sarkar, D., Datta, D., Sen, D., Bhattacharjee, C. Simulation of continuous stirred rotating disk-membrane module: An approach based on surface renewal theory. *Chemical Engineering Science*, **2011**, 66(12), 2554-2567.
[2] Nourmohamadi, H., Fazlavi, A., Keyvan, S. Modeling cobalt ion adsorption with synthesized magnetite bentonite (smb) nano-absorbent: By ccd. *Iranian Journal of Chemistry and Chemical Engineering*, **2021**, 40(5), 1532-1540.
[3] Shannon, M.A., Bohn, P.W., Elimelech, M., Georgiadis, J.G., Mariñas, B.J., Mayes, A.M. Science and technology for water purification in the coming decades. *Nature*, **2008**, 452(7185), 301-310.
[4] Asatekin, A., Mayes, A.M. Oil industry wastewater treatment with fouling resistant membranes containing amphiphilic comb copolymers. *Environmental Science & Technology*, **2009**, 43(12), 4487-4492.
[5] Robertson, S.J., McGill, W.B., Massicotte, H.B., Rutherford, P.M. Petroleum hydrocarbon contamination in boreal forest soils: A mycorrhizal ecosystems perspective. *Biological Reviews*, **2007**, 82(2), 213-240.
[6] Padaki, M., Murali, R.S., Abdullah, M.S., Misdan, N., Moslehyani, A., Kassim, M., Hilal, N., Ismail, A. Membrane technology enhancement in oil–water separation. A review. *Desalination*, **2015**, 357, 197-207.
[7] Kota, A.K., Kwon, G., Choi, W., Mabry, J.M., Tuteja, A. Hygro-responsive membranes for effective oil–water separation. *Nature Communications*, **2012**, 3(1), 1025.
[8] Zhang, W., Liu, N., Cao, Y., Chen, Y., Xu, L., Lin, X., Feng, L. A solvothermal route decorated on different substrates: Controllable separation of an oil/water mixture to a stabilized nanoscale emulsion. *Advanced Materials (Deerfield Beach, Fla.)*, **2015**, 27(45), 7349-7355.
[9] Kong, J., Li, K. Oil removal from oil-in-water emulsions using pvdf membranes. *Separation and Purification Technology*, **1999**, 16(1), 83-93.
[10] Abadi, S.R.H., Sebzari, M.R., Hemati, M., Rekabdar, F., Mohammadi, T. Ceramic membrane performance in microfiltration of oily wastewater. *Desalination*, **2011**, 265(1-3), 222-228.
[11] Cheryan, M., Rajagopalan, N. Membrane processing of oily streams. Wastewater treatment and waste reduction. *Journal of Membrane Science*, **1998**, 151(1), 13-28.

[12] Rahimpour, A., Madaeni, S.S., Mansourpanah, Y. Nano-porous polyethersulfone (pes) membranes modified by acrylic acid (aa) and 2-hydroxyethylmethacrylate (hema) as additives in the gelation media. *Journal of Membrane Science*, **2010**, 364(1-2), 380-388.
[13] Singh, V., Purkait, M., Das, C. Cross-flow microfiltration of industrial oily wastewater: Experimental and theoretical consideration. *Separation Science and Technology*, **2011**, 46(8), 1213-1223.
[14] El Jery, A., Ahsan, A., Sammen, S.S., Shanableh, A., Sain, D., Ramírez-Coronel, A.A., Uddin, M.A., Maktoof, M.A.J., Shafiquzzaman, M., Al-Ansari, N. Industrial oily wastewater treatment by microfiltration using silver nanoparticle-incorporated poly (acrylonitrile-styrene) membrane. *Environmental Sciences Europe*, **2023**, 35(1), 64.
[15] Liu, J., Wang, L., Wang, N., Guo, F., Hou, L., Chen, Y., Zhao, Y., Jiang, L. A robust Cu $(OH)_2$ nanoneedles mesh with tunable wettability for nonaqueous multiphase liquid separation. *Small (Weinheim an der Bergstrasse, Germany)*, **2016**, 13(4).
[16] Liu, N., Zhang, Q., Qu, R., Zhang, W., Li, H., Wei, Y., Feng, L. Nanocomposite deposited membrane for oil-in-water emulsion separation with in situ removal of anionic dyes and surfactants. *Langmuir*, **2017**, 33(30), 7380-7388.
[17] Yang, H.C., Luo, J., Lv, Y., Shen, P., Xu, Z.K. Surface engineering of polymer membranes via mussel-inspired chemistry. *Journal of Membrane Science*, **2015**, 483, 42-59.
[18] Wei, W., Sun, M., Zhang, L., Zhao, S., Wu, J., Wang, J. Underwater oleophobic PTFE membrane for efficient and reusable emulsion separation and the influence of surface wettability and pore size. *Separation and Purification Technology*, **2017**, 189, 32-39.
[19] He, Y., Jiang, Z.W. Technology review: Treating oilfield wastewater. *Filtration & Separation*, **2008**, 45(5), 14-16.
[20] Mansourizadeh, A., Javadi Azad, A. Preparation of blend polyethersulfone/cellulose acetate/polyethylene glycol asymmetric membranes for oil–water separation. *Journal of Polymer Research*, **2014**, 21(3), 375.
[21] Ochoa, N.A., Masuelli, M., Marchese, J. Effect of hydrophilicity on fouling of an emulsified oil wastewater with pvdf/pmma membranes. *Journal of Membrane Science*, **2003**, 226(1-2), 203-211.
[22] Rahimpour, A., Madaeni, S.S. Polyethersulfone (pes)/cellulose acetate phthalate (cap) blend ultrafiltration membranes: Preparation, morphology, performance and antifouling properties. *Journal of Membrane Science*, **2007**, 305(1-2), 299-312.
[23] Beach, E., Brown, S., Shqau, K., Mottern, M., Warchol, Z., Morris, P. Solvothermal synthesis of nanostructured NiO, ZnO and CO_3O_4 microspheres. *Materials Letters*, **2008**, 62(12-13), 1957-1960.
[24] Pandey, S. A comprehensive review on recent developments in bentonite-based materials used as adsorbents for wastewater treatment. *Journal of Molecular Liquids*, **2017**, 241, 1091-1113.
[25] Yuliwati, E., Ismail, A. Effect of additives concentration on the surface properties and performance of pvdf ultrafiltration membranes for refinery produced wastewater treatment. *Desalination*, **2011**, 273(1), 226-234.
[26] Ong, C., Lau, W., Goh, P., Ng, B., Ismail, A. Preparation and characterization of PVDF–PVP–TiO_2 composite hollow fiber membranes for oily wastewater treatment using submerged membrane system. *Desalination and Water Treatment*, **2015**, 53(5), 1213-1223.
[27] Zangeneh, H., Zinatizadeh, A.A., Zinadini, S. Self-cleaning properties of l-histidine doped TiO_2-CDS/PES nanocomposite membrane: Fabrication, characterization and performance. *Separation and Purification Technology*, **2020**, 240, 116591.
[28] Ong, C., Lau, W., Goh, P., Ng, B., Ismail, A. Investigation of submerged membrane photocatalytic reactor (smpr) operating parameters during oily wastewater treatment process. *Desalination*, **2014**, 353, 48-56.
[29] Nakakita, K., Akihama, K., Weissman, W., Farrell, J. Effect of the hydrocarbon molecular structure in diesel fuel on the in-cylinder soot formation and exhaust emissions. *International Journal of Engine Research*, **2005**, 6(3), 187-205.
[30] Ogawa, H., Nishimoto, H., Morita, A., Shibata, G. Predicted diesel ignitability index based on the molecular structures of hydrocarbons. *International Journal of Engine Research*, **2016**, 17(7), 766-775.
[31] Mueller, C.J., Cannella, W.J., Bays, J.T., Bruno, T.J., DeFabio, K., Dettman, H.D., Gieleciak, R.M., Huber, M.L., Kweon, C.-B., McConnell, S.S. Diesel surrogate fuels for engine testing and chemical-kinetic modeling: Compositions and properties. *Energy & Fuels*, **2016**, 30(2), 1445-1461.
[32] Benkhaya, S., Lgaz, H., Alrashdi, A.A., M'rabet, S., El Bachiri, A., Assouag, M., Chung, I.-M., El Harfi, A. Upgrading the performances of polysulfone/polyetherimide ultrafiltration composite membranes for dyes removal: Experimental and molecular dynamics studies. *Journal of Molecular Liquids*, **2021**, 331, 115743.
[33] Bope, C.D., Nalaparaju, A., Ng, C.K., Cheng, Y., Lu, L. Molecular simulation on the interaction of

ethinylestradiol (EE2) with polymer membranes in wastewater purification. *Molecular Simulation*, **2018**, 44(8), 638-647.
[34] Golzar, K., Amjad-Iranagh, S., Amani, M., Modarress, H. Molecular simulation study of penetrant gas transport properties into the pure and nanosized silica particles filled polysulfone membranes. *Journal of Membrane Science*, **2014**, 451, 117-134.
[35] Luo, Y., Liu, Z., Liu, Y., Huang, J., Zhang, M., Molecular dynamics coupled with experimental study of the effects of polyethylene glycol on the structure and antifouling properties of polyethersulfone membranes. *Journal of Applied Polymer Science*, **2023**, 140(36), e54364.
[36] Wang, M., Wang, J., Jiang, J. Membrane fouling: Microscopic insights into the effects of surface chemistry and roughness. *Advanced Theory and Simulations*, **2022**, 5(1), 2100395.
[37] Delley, B. An all-electron numerical method for solving the local density functional for polyatomic molecules. *The Journal of Chemical Physics*, **1990**, 92(1), 508-517.
[38] Delley, B. From molecules to solids with the dmol 3 approach. *The Journal of Chemical Physics*, **2000**, 113(18), 7756-7764.
[39] Klamt, A., Schüürmann, G. Cosmo: A new approach to dielectric screening in solvents with explicit expressions for the screening energy and its gradient. *Journal of the Chemical Society, Perkin Transactions 2*, **1993**, (5), 799-805.
[40] Rappe, A., Colwell, K., Casewit, C. Application of a universal force field to metal complexes. *Inorganic Chemistry*, **1993**, 32(16), 3438-3450.
[41] Shuichi, N. Constant temperature molecular dynamics methods. *Progress of Theoretical Physics Supplement*, **1991**, 103, 1-46.
[42] Nourmohamadi, H., Esrafili, M.D., Aghazadeh, V., Rezai, B. The influence of Ag^{+} cation on elemental sulfur passive layer and adsorption behavior of chalcopyrite toward Fe^{3+} and Fe^{2+} ions: Insights from dft calculations and molecular dynamics simulations. *Physica B: Condensed Matter*, **2022**, 627, 413611.
[43] Aghazadeh, V., Rezai, B., Nourmohamadi, H. A thermodynamic investigation of the interaction of ferric (Fe^{3+}) ion with (100, 110) pyrite and (001) chalcopyrite surfaces using the density functional theory study. *Advanced Journal of Chemistry-Section A*, **2023**, 6(3), 301-310.
[44] Nourmohamadi, H., Esrafili, M.D., Aghazadeh, V. Interaction of ferric ion with (001)-s and (001)-m surfaces of chalcopyrite (M= Fe and Cu): Electrochemical insights from DFT calculations. *Applied Surface Science*, **2019**, 495, 143529.
[45] Zhang, N., Yang, X., Wang, Y., Qi, Y., Zhang, Y., Luo, J., Cui, P., Jiang, W. A review on oil/water emulsion separation membrane material. *Journal of Environmental Chemical Engineering*, **2022**, 10(2), 107257.
[46] Sahu, L.R., Yadav, D., Borah, D., Gogoi, A., Goswami, S., Hazarika, G., Karki, S., Borpatra Gohain, M., Sawake, S.V., Jadhav, S.V. Polymeric membranes for liquid separation: Innovations in materials, fabrication, and industrial applications. *Polymers*, **2024**, 16(23), 3240.

HOW TO CITE THIS ARTICLE

H. Nourmohamadi, R.S. Neyband. Theoretical Simulation of Oil Pollutant Adsorption: Diesel Interactions with Polyethersulfone Membranes. *Adv. J. Chem. A*, 2026, 9(7), 1337-1347.

DOI: 10.48309/AJCA.2026.526710.1910
URL: https://www.ajchem-a.com/article_241028.html